Accepted Manuscript

Aptamer-Based Biosensor for Label-free Detection of Ethanolamine by Electrochemical Impedance Spectroscopy

Gang Liang, Yan Man, Xinxin Jin, Ligang Pan, Xinhui Liu

PII: S0003-2670(16)30819-4

DOI: 10.1016/j.aca.2016.06.056

Reference: ACA 234680

To appear in: *Analytica Chimica Acta*

Received Date: 1 April 2016

Revised Date: 28 June 2016

Accepted Date: 30 June 2016

Please cite this article as: G. Liang, Y. Man, X. Jin, L. Pan, X. Liu, Aptamer-Based Biosensor for Label-free Detection of Ethanolamine by Electrochemical Impedance Spectroscopy, *Analytica Chimica Acta* (2016), doi: 10.1016/j.aca.2016.06.056.

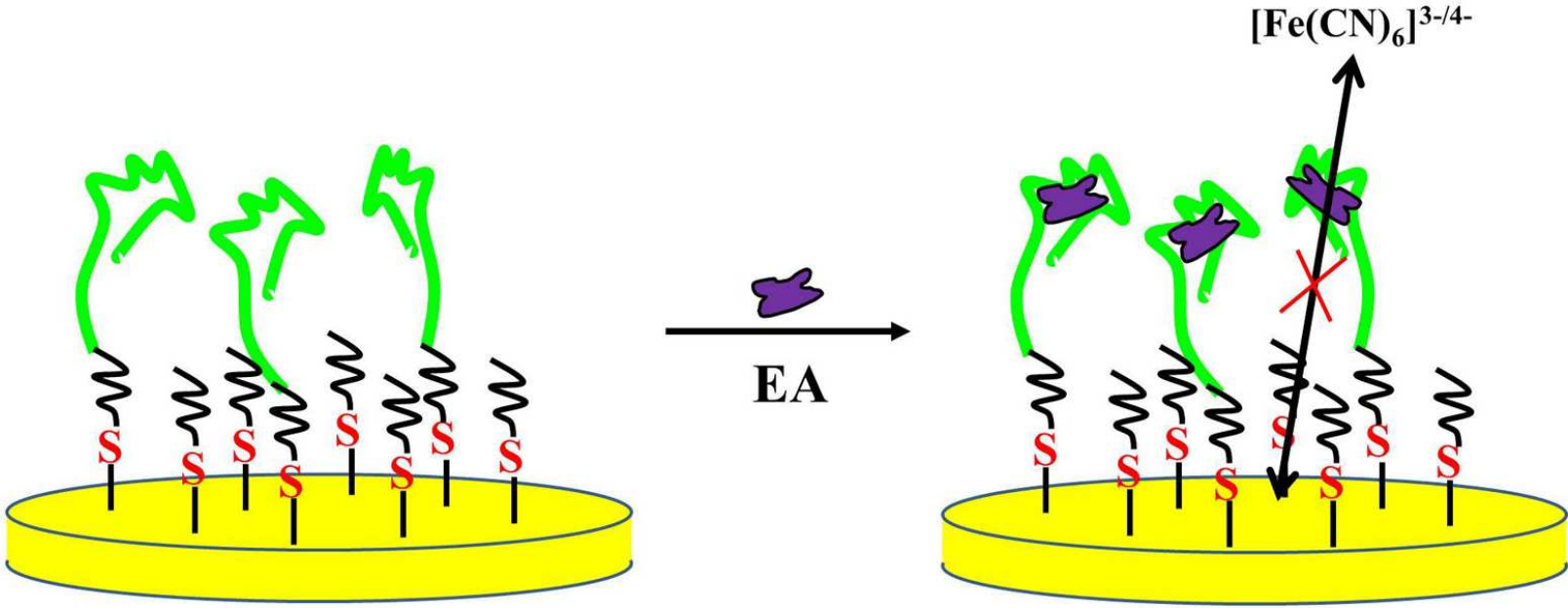

Aptamer-Based Biosensor for Label-free Detection of Ethanolamine by Electrochemical Impedance Spectroscopy

Gang Liang[a,b], Yan Man[a], Xinxin Jin[a], Ligang Pan[a*] and Xinhui Liu[b*]

[a] *Risk Assessment Lab for agro-products (Beijing), Ministry of Agriculture P. R. China and Beijing Municipal Key Laboratory of Agriculture Environment Monitoring, Beijing Research Center for Agricultural Standards and Testing, Beijing Academy of Agricuture and Forestry Science, Beijing 100097 P. R. China*

[b] *State Key Laboratory of Water Environment Simulation, School of Environment, Beijing Normal University, Beijing 100875, P. R. China*

[*]Corresponding Authors: xhliu@bnu.edu.cn (Xinhui Liu), Tel./Fax: +86-01-58802996

panlg@nercita.org.cn (Ligang Pan), Tel.: +86-01-51503729

Abstract:

A label-free sensing assay for ethanolamine (EA) detection based on G-quadruplex-EA binding interaction is presented by using G-rich aptamer DNA (Ap-DNA) and electrochemical impedance spectroscopy (EIS). The presence of K^+ induces the Ap-DNA to form a K^+-stabilized G-quadruplex structure which provides binding sites for EA. The sensing mechanism was further confirmed by circular dichroism (CD) spectroscopy and EIS measurement. As a result, the charge transfer resistance (R_{CT}) is strongly increased as demonstrated by using the ferro/ferricyanide ($[Fe(CN)_6]^{3-/4-}$) as a redox probe. Under the optimized conditions, a linear relationship between ΔR_{CT} and EA concentration was obtained over the range of 0.16 nM and 16 nM EA, with a detection limit of 0.08 nM. Interference by other selected chemicals with similar structure was negligible. Analytical results of EA spiked into tap water and serum by the sensor suggested the assay could be succesfully applied to real sample analysis. With the advantages of high sensitivity, selectivity and simple sensor construction, this method is potentially suitable for the on-site monitoring of EA contamination.

Key words:

Aptamer; Biosensor; Ethanolamine; Electrochemical impedance spectroscopy

1. Introduction

Organic amines are a class of ubiquitous environmental contaminants with high mutagenicity, teratogenicity and carcinogenicity [1, 2]. The carcinogenesis of the amines is mainly due to the highly reactive and electrophilic intermediates produced by N-hydroxylation of the amine group in metabolic activation process [3, 4], as the produced intermediates can interact with nucleobases to form DNA adducts and produce different types of lesions [5, 6], which can induce mutation in the process of DNA replication and transcription, and finally initiating cancer disease [7]. Ethanolamine (EA), one of the smallest molecules of aliphatic amine with simple structure, plays very important roles in textile, chemical industries, pharmaceuticals, biology science, and has been widely used in the production of dyes and pesticides intermediates, insecticide, medicine, adhesives, rubber-manufacturing processes (rubber accelerator, vulcanizing agent of the rubber) and surfactant. However, studies showed that human exposure to EA can irritate the skin, eyes and cause damage to the respiratory tract [8]. Furthermore, EA can also inhibit the nervous system when it entered the human body. Besides, it's confirmd that EA is associated with Alzheimer's disease [9], Schizophrenia [10], and the carcinogenic activity of EA is investigated as well [11]. So it is necessary to develop efficient methods for the determination of EA.

Commonly, high-performance liquid chromatography (HPLC) with UV and/or fluorescence detection method is the thchnique that widely used for detection of small molecules [11]. However, these methods are relatively complicated; require expensive equipments, time-consuming pre-treatment of the sample prior to analysis, highly qualified technicians and a

laboratory environment. Under this situation, an achievement of simple and cost-effective assay is imperative [12]. Electrochemical technique is an interesting and convenient alternative that has allowed one to simplify the detection process [13], and is ease to miniaturize resulting in low consumption of nucleic acid aptamers [14]. Especially, the interaction between DNA and the target molecules provides the basis for analytical devices in laboratory [15]. So electrochemical DNA sensors possess enormous potential for the task of rapid, simple and sensitive detection of target molecules [16, 17] due to their convenience, high selectivity and sensitivity. And electrochemical impedance spectroscopy (EIS) has been proven to be a most powerful and sensitive tool for probing the features of surface-modified electrodes [18]. EIS biosensors possess unique advantages, such as the ability to separate the surface binding events from the solution impedance, ease of signal quantification, less damage to the biological interactions being measured, and the possibility to use non-labeled DNA [19].

Up to date, little efforts have been given to develop DNA sensors for amine compounds, and only a few DNA sensor for the detection of the aromatic amines based on the binding interaction have been reported [20, 21]. For example, Liang et al. reported a hairpin DNA modified sensor for the electrochemical determination of amino-substituted naphthalene compounds with high sensitivity, and further confirmed the binding mode of the aminonaphthalenes with hairpin DNA [12]. However, all these electrochemical DNA sensors showed poor selectivity to the target amine compounds, and can not discriminate between different amine componds. So developing sensors for amine compounds with high selectivity is still of a great challenge.

In contrast, aptamer exhibits high affinity to specific targets. Thus, aptamers become important components in the design of biosensors, and aptamer-based sensors have been widely usded for targeting small molecule [22], such as cocaine [23], organophosphorus pesticides [24, 25], heavy metals [26], pharmaceuticals [27, 28], due to the considerable advantages, such as thermal stability, simpler preparation, lower-priced production cost, high selectivity and sensitivity for targets [22, 29]. Until now, EA aptamer, one of the smallest aptamer targets so far, has been in vitro-selected [30], but few aptamer sensors have been constructed for EA detection. On the basis of the findings, Heilkenbrinker group reported an aptamer-based microarray assay based on competition between EA and the fluorescein-labeled DNA strand, which is complementary to the aptamer DNA sequence immobilized on the microarray surface [11]. This methods made great improvements in detection techniques for EA. However, the signal-off fluorescent sensor has a major drawback in that the fluorescence signal can be easily affected by matrixes existed in the testing system, which limit the scope of their applications in environmental and biological samples. Therefore, it still remains a challenge to achieve simple, cost-effective, label-free determination of EA with high capacity of resisting disturbance, which could really meet the requirements for EA detection in real samples. So developing aptamer DNA-based sensors with high specificity, sensitivity is of great significance.

In the present work, a label-free sensing assay for the detection of EA was reported based on aptmer DNA (Ap-DNA) sensor by electrochemical impedance spectroscopy (EIS). Simply, a hairpin Ap-DNA was first immobilized on the gold electrodes and transformed into G-quadruplex, which can bind with EA. The interaction mechanism was further confirmed by

circular dichroism (CD) spectroscopy and EIS. Depending on the difference of charge transfer resistance change (ΔR_{CT}) before and after reaction with EA, EA can be sensitively and selectively detected with a detection limit of 0.08 nM in buffer solution. Finally, the Ap-DNA assay was successfully performed in natural tap water and serum samples.

2. Materials and methods

2.1 Materials

The following DNA sequences (the thiolated arbitrary single-stranded DNA and aptamer DNA of EA) were purchased from Shanghai Sangon Biological Engineering Technology & Service Co. Ltd (http://www.sangon.com).

5'-HS-$(CH_2)_6$-TTTTTTTATTCAAGAGGTGGGT-3' (ss-DNA)

5'-HS-$(CH_2)_6$-TTTTTTTATTCAA**TTTGAGGCGGGTGGGTGGG**TTGAATA-3' (Ap-DNA)

6-Mercapto-1-hexanol (MCH), $NaClO_4$, Tris (tris-(hydroxymethyl)-aminomethane) (Tris), tris (2-carboxyethyl) phosphine hydrochloride (TCEP), $K_3[Fe(CN)_6]$, $K_4[Fe(CN)_6]$, EDTA, KCl, $MgCl_2$, $[Ru(NH_3)_6]Cl_2$, $[Ru(NH_3)_6]Cl_3$ were purchased from Sigma-Aldrich (http://www.sigmaaldrich.com/china-mainland.html) and used without further purification. Ethanolamine (EA), ethanol, glycol, isopropanol, isopropanolamine (IPA), HCl, $HClO_4$, NaCl, $CaCl_2$ were purchased from Sinopharm Chemical Reagents Beijing Co., Ltd (http://www.crc-bj.com). Fetal calf serum (FBS) was obtained from JIBCO (Cat: 10099-141, Invitrogen, MA, USA). The working gold electrodes, 99.99% (w/w) polycrystalline with a diameter 1 mm, were obtained from Aida Instrument Inc. in Tianjin (China) (http://www.tjaida.cn) and cleaned prior to use as reported before.

The stock solutions of thiolated DNA (10 μM) was prepared in Tris-HCl buffer (20 mM, pH=7.4) and then heated at 80 ℃ for 5 min to remove possible DNA aggregates and to dissociate any intermolecular interaction, obtaining uniform single-standed DNA solution and gradually cooled to room temperature prior to use [19]. And then, the DNA stock solution was diluted to a final concentration of 1 μM with the DNA immmobilization buffer (10 mM Tris-HCl, 1.0 M NaCl, 1mM EDTA, 1 mM TCEP, pH 8.0). TCEP was used to cleave disulfides. Besides, the Tris-HCl buffer (20 mM, pH=7.6) containing 100 mM NaCl, 5 mM KCl, 2 mM $MgCl_2$, 1 mM $CaCl_2$, 0.02% Tween was prepared and used as binding buffer (B-buffer) for Ap-DNA and EA. EA was diluted with B-buffer to obtain a series of EA solutions with different concentration prior to use. Serum sample was prepared by diluting with B-buffer with a final concentration of 10% serum, and then for EA solution preparation. Tap water was first purified with the filter membrane (0.45 μm), then used to prepare "B-buffer" instead of Milli-Q water. The prepared "B-buffer" was applied for EA solution preparation. All other solutions were prepared with Milli-Q water (18.2 MΩ cm resistivity) from a Millipore Milli-Q system (Thermo Scientific EASYpure II).

2.2 **Fabrication of the DNA sensor**

The gold electrodes were cleaned prior to thiolated DNA modification as reported before [19]. Briefly,the gold electrodes were first mechanically polished on a microcloth (Buehler) with Gamma alumina (0.05 μm) slurries, followed by successive sonication in ethanol and Milli-Q water for 5 min. Then, the electrodes were electrochemically cleaned in 1 mol L^{-1} H_2SO_4 by cyclic voltammetry (CV) (0-1.5 V *vs* Ag/AgCl) cycling to remove any remaining surface

impurities. After thoroughly rinsed with Milli-Q water, the gold electrodes were blown-dry with a nitrogen gun, and ready for DNA modification. The DNA modified films were prepared by incubating the freshly cleaned gold electrodes in the prepared DNA solutions (1 μM), followed by backfilling potential pinholes and defects by soaking the DNA films in 1 mM 6-mercaptohexanol for 1h. Then the electrodes were washed with Tris-HCl buffer (20 mM, pH=7.4) and mounted into an electrochemical cell for impedimetric measurements. After rinsing with buffer again, the preprared sensors were incubated in B-buffer for 2h. Finally, the prepared sensors were ready for EA detection (each sensor can be used only once), and EIS of the sensor was recorded. Rinsing each layer of the electrode for 30s with buffer before EIS measurement and all EIS experiments were conducted at 25 ℃ in Tris-$NaClO_4$ (20 mM, pH=7.4) buffer solution.

2.3 **Electrochemical measurements**

Electrochemical experiment for Electrochemical Impedance Spectroscopy (EIS) and Chronocoulometry (CC) was carried out on a CHI 650D electrochemical workstation (Shanghai Chenhua instrument Co. Ltd., China). As reported before [12], a conventional three-electrode system was used. The DNA modified gold electrode was employed as the working electrode. The reference electrode was constructed by sealing an Ag/AgCl wire into a glass tube with a solution of saturated KCl that was capped with a Vycor tip. The counter electrode was a platinum wire.

The ac voltage amplitude was 5 mV, and the voltage frequencies used for EIS measurements ranged from 100 kHz to 100 mHz. The applied potential was 250 mV *vs.*

Ag/AgCl (formal potential of the redox probe $[Fe(CN)_6]^{3-/4-}$ in the buffer solution).

CC measurements were successively performed in Tris-$HClO_4$ (20 mM, pH=7.4) and 100 μM $[Ru(NH_3)_6]^{3+}$ Tris-$HClO_4$ (20 mM, pH=7.4) buffer solution. The test solutions were firstly bubbled thoroughly with high purity nitrogen for 10 min prior to CC measurement. The following parameters were employed for CC: pulse period = 500 ms, pulse width = 500 mV.

All measurements were repeated for a minimum of three times with separate electrode to obtain the statistically meaningful result. All experiments were performed at room temperature.

2.4 **Circular dichroism measurement**

Circular dichroism (CD) spectra were measured with a Jasco J-810 spectropolarimeter at room temperature. The 25 μM DNA solution was prepared in Tris-HCl buffer (20 mM, pH=7.4) and B-buffer, respectively. Subsequently, added to this B-buffer solution was 25 μM EA for 2h. The spectra were accumulated and averaged from three scans recorded from 200 nm to 400 nm at 0.5 nm intervals with an scan rate of 200 nm min^{-1}.

3. Results and discussion

3.1 EA Sensing Principle

<**Scheme 1**>

A schematic diagram illustrating the sensing principle was shown in Scheme 1. The designed label-free aptamer DNA sequence, in which the underlined bases are complementary pairs, can self-assemble into hairpin structure with a stable stem near the 5’-end. The G-rich sequence (bold bases), which is located in the single-stranded loop, can form a G-quadruplex strcture in B-buffer solution and then capture EA serving as the binding site [11]. The specific

binding interaction of EA and G-quadruplex, forming EA/G-quadruplex complex, resulted in the charge-transfer resistance (R_{CT}) increase between the solution-based redox probe $[Fe(CN)_6]^{3-/4-}$ and the electrode surface. The increase of ΔR_{CT} ($\Delta R_{CT}=R_{CT(after)}-R_{CT(before)}$) is positive related to the EA level, and the determination of EA can be achieved.

3.2 Demomstration of the principle

< **Fig. 1**>

As for the proposed mechanism, CD spectra were first applied to investigate the conformational switches of the Ap-DNA. As shown in Fig. 1, the designed Ap-DNA showed a negative peak at 246 nm and a positive peak around 275 nm in Tris-HCl (20 mM, pH=7.4) (curve a), which was indicative of the formation of a stem-loop structure (hairpin DNA) [31]. And no obvious CD change was observed when incubating the Ap-DNA in Tris-HCl (20 mM, pH=7.4) buffer containing EA (curve b), suggesting that the presence of EA can not destroy the formed stem-loop structure. In contrast, incubation in B-buffer of the Ap-DNA displayed a blue shift of the negative and positive band with significantly increased intensity. And the Ap-DNA exhibited a strong positive peak at 266 nm and a negative peak at 242 nm (curve c), which was indicative of parallel K^+-stabilized G-quadruplex [32, 33]. The results demonstrated that the presence K^+ could induce the hairpin Ap-DNA structural change, forming K^+-stabilized G-quadruplex. However, only a very small CD change was observed when adding EA to the K^+-stabilized G-quadruplex system (curve d), which is negligible compared to that of the Ap-DNA/K^+ system, suggesting no further G-quadruplex structural change was induced by EA. Therefore, we can inferred that K^+-stabilized G-quadruplex is essential for EA detection,

offering the binding site of EA [11].

Subsequently, EIS mesurements were carried out to confirm the sensing principle on the electrode. First, the Ap-DNA films were prepared by incubating the freshly cleaned gold electrodes in the prepared 1 μM Ap-DNA solution for 6 h (see supporting information Fig. S1). Then, the prepared Ap-DNA films were incubated in B-buffer solution for 2 h, and the Ap-DNA was transformed into G-quadruplex complex on the electrode surface. EIS was applied to track the processes and the representative Nyquist plots for the corresponding films were shown Fig. S2 (see Supporting Information). The impedance spectra for all the systems were analyzed with the help of a modified Randles' equivalent circuit (inset of Fig. S2) [34]. As shown in Fig. S2, a large R_{CT} increase was observed when the prepared Ap-DNA films were incubated in B-buffer solution for 2 h, revealing that the Ap-DNA was transformed into G-quadruplex on the electrode surface. This is because the formed K^+-stabilized G-quadruplex had a higher space charge density than the Ap-DNA that enhanced the repulsion of the redox probe $[Fe(CN)_6]^{3-/4-}$ [35]. To further confirm this transformation, the positive redox probe of $[Ru(NH_3)_6]^{2+/3+}$ was also applied for EIS measurement as shown in Fig. S3.

< **Fig. 2**>

Next, the specific interaction between the formed G-quadruplex and EA was further confirmed. The representative Nyquist plots of the binding interaction between G-quadruplex films with 1.6 mM EA were shown in Fig. 2. As shown in Fig. 2, the R_{CT} significantly increased after incubating the G-quadruplex films in EA solution for 1h (optimization of incubation time shown in Fig. S4), indicating the specific binding interaction between the formed G-quadruplex

and EA. This can be rationalized that the formed G-quadruplex on the electrode surface can provide binding sites for EA, forming EA/G-quadruplex complex [11], which hinders the electron transfer [36], resulting in an increased R_{CT}.

Until now, a question maybe raised: wheather EA can interact with single strand DNA (ss-DNA) modified DNA films? EIS measurement was applied to evaluate the interaction effect of ss-DNA with EA with the concentration of 1.6 mM. To confirm this, an arbitrary ss-DNA was immobilized on the gold electrodes and then applied to investigate the interaction with EA (the same precedure as the Ap-DNA film). The representative Nyqiust plots were analyzed with the equivalent circuit (inset of Fig. 2) and the corresponding ΔR_{CT} were obtained as shown in Fig. S5 (see supporting information). As shown in Fig. S5, however, only a very small increase of R_{CT} was observed over the same period when the ss-DNA film was utilized, and the ΔR_{CT} was about 17.3 (2.8) $\Omega \cdot cm^2$, which was negligible in contrast to the ΔR_{CT} of Ap-DNA film induced by EA. Hence, it was reasonably concluded that the significantly increased ΔR_{CT} of the Ap-DNA film was indeed due to the specific interaction of EA with the G-quartet binding site.

Based on the results discussed above, it can be concluded that: (1) the thiolated Ap-DNA was self-assembled on the gold electrodes via the strong covalent Au-S bond; (2) the immobilized hairpin Ap-DNA folds into G-quadruplex structure when incubated in B-buffer; (3) the formed G-quadruplex of Ap-DNA, which acts as the EA binding sites, can capture EA onto the electrode surface, as shown in Scheme 1. Due to the binding interaction with EA, R_{CT} of the G-quadruplex film was significantly increased. As a result, with Ap-DNA as a sensing probe, the ΔR_{CT} as an electrochemical signal was applied for the detection of EA.

3.3 Electrochemical detection of EA

Based on the sensing mechanism, Ap-DNA was applied as a probe to immobilize on the gold electrodes for electrochemical detection of EA by EIS. The freshly prepared G-quadruplex modified electrodes were immersed into EA/B-buffer solutions for 1h. The representative Nyquist plots of the binding interaction between G-quadruplex films with 1.6 mM EA were shown in Fig. 2. The impedance spectra were analyzed with the modified Randles' equivalent circuit (inset of Fig. 2) [34], and the fitting results were listed in Table 1.

<**Table 1**>

The solution resistance, R_s, is the resistance between the reference electrode and the G-quadruplex films of Ap-DNA immobilized on the working electrodes, which ranged from 4.4 (0.2) $\Omega \cdot cm^2$ to 5.4 (0.2) $\Omega \cdot cm^2$. C_{film} accounts for the capacitance of the Ap-DNA films on the gold electrodes. As shown in Table 1, C_{film} was decreased after immersing the Ap-DNA films in EA solution, revealing that the interaction on the Ap-DNA film might lead to an increase in the film thickness that resulted in a decreased dielectric constant [35]. The combination of R_x and the constant phase element (CPE) accounts for the behavior of the 6-mercaptohexanol groups on the electrode surfaces [36, 37]. CPE acts as a nonlinear capacitor accounting for the inhomogeneity of the films on the electrode surface with the exponential modifier n = 0.9 [38, 39]. Mass transport is not a major contributor because of the absence of Warburg impedance as shown in Fig. 1.

The most important parameter is the charge-transfer resistance (R_{CT}) [40], which is the result of the resistance to charge transfer between the solution-based redox probe $[Fe(CN)_6]^{3-/4-}$

and the electrode surface. As shown in Table 1, after incubating the G-quadruplex Ap-DNA films with 1.6 mM EA solution for 1h, the R_{CT} significantly increased from 1190.8 (59.7) $\Omega \cdot cm^2$ ($R_{CT(before)}$) to 1603.7 (75.3) $\Omega \cdot cm^2$ ($R_{CT(after)}$) and the ΔR_{CT} was about 412.9 (27.4) $\Omega \cdot cm^2$. Therefore, the ΔR_{CT} was a very significant parameter to be applied for the detection of EA.

<**Fig. 3**>

Susequently, we investigated the relationship between the ΔR_{CT} of the Ap-DNA films and the concentrations of EA with the concentrations ranged from 0.08 nM to 1.6 mM. As shown in Fig. 3A, the ΔR_{CT} was sharply increased with increasing the concentration of EA from 0.08 nM to 1.6 mM, until the inflection point appeared when the EA concentration reached 160 nM, suggesting that the higher EA concentration was used, the more G-quadruplex/EA complexs formed on the electrode. After that, the ΔR_{CT} changed slowly with the increased EA concentration from 160 nM to 1.6 mM, whereas upon decreasing the concentration of EA to 0.08 nM, no distinct ΔR_{CT} change was observed compared to that in buffer solution, which was due to the less G-quadruplex/EA complexs formed on the electrode films. And the detection limit was determined to be 0.08 nM, which is comparable to the fluorescent assay for EA (0.01 nM) [11] and much lower than that of chromatographic methods as shown in Table S1. Fig. 3B showed the linear dependance between ΔR_{CT} and the concentrations of EA in the range of 0.16 nM to 16 nM, and the regression equation was $Y(\Delta R_{CT})=60.6+5.4X(C_{EA})$ with a correlation coefficient of 0.97.

3.4 Selectivity and stability of the sensor

< **Fig. 4**>

Selectivity is one of the significant performances of the biosensor, so the selectivity of the Ap-DNA sensor was exploited by measuring the ΔR_{CT} of the Ap-DNA films in the presence of other chemicals with similar structure, such as 1.6 μM ethanol, glycol, isopropanol and isopropanolamine (IPA), respectively. As shown in Fig. 4, EA caused a considerable increase in ΔR_{CT} ($\Delta R_{CT}=R_{CT(after)}-R_{CT(blank)}$), while even with 100 times excess of other selected compounds, the ΔR_{CT} was substantially lower than with EA. This excellent selectivity could be attributed to the highly specific binding interaction of G-quadruplex with EA. Compared with the homogeneous assays such as fluorescent methods, one advantage of the electrochemical Ap-DNA sensors is that it suffers less environmental interference, for the electrodes can be rinsed before every operation step, which also avoids the worry that the fluorescent signal may be quenched by other coexisting compounds. The excellent ability of the Ap-DNA sensor to discriminate EA from other chemicals by EIS added a new and important dimension of selectivity.

Furthermore, we also investigated the stablity of the Ap-DNA film. As shown in Fig. S6, after incubating the G-quadruplex films with 160 nM EA solution for 1h, the R_{CT} significantly increased and the ΔR_{CT} was about 339.5 (13.9) $\Omega \cdot cm^2$. However, no significant ΔR_{CT} loss was observed when the Ap-DNA film was incubated in B-buffer at 4 ℃ even for 7 days (305.1 (24.5) $\Omega \cdot cm^2$). The results demonstrated that a stable Ap-DNA film formed on the gold electrode due to the Au-S covalent bonding. Besides, very small uncertainty values (Error bar) were obtained, varied from 4.1% to 8.0%, demonstrating good reliability of the sensor.

3.5 Application in real samples

<Fig. 5>

Finally, in view of the importance of EA detection in real samples, the performance of the Ap-DNA sensor was also challenged in tap water and serum samples. As shown in Fig. 5, after incubating the Ap-DNA sensor in serum samples containing EA 16 nM, 160 nM and 1600 nM, the R_{CT} of the Ap-DNA films significantly increased and the ΔR_{CT} were 122.7 (1.7) $\Omega \cdot cm^2$, 308.9 (27.5) $\Omega \cdot cm^2$ and 318.7 (38.9) $\Omega \cdot cm^2$, respectively, which was comparable as that obtained in B-buffer solution. Similarly, a continuously increased ΔR_{CT} was observed as well when immersing the Ap-DNA sensor in tap water sample containing EA of 16 nM, 160 nM and 1600 nM, and the ΔR_{CT} were 136.2 (7.8) $\Omega \cdot cm^2$, 319.9 (17.4) $\Omega \cdot cm^2$ and 339.7 (18.7) $\Omega \cdot cm^2$, respectively. The results implied that the designed electrochemical Ap-DNA sensor can be efficiently applied to recognize EA in tap water and serum samples for further environmental and biomedical application.

4. Conclusion

To conclude, a label-free sensing assay has been developed for ethanolamine (EA) detection by electrochemical impedance spectroscopy. The sensor employed a G-rich aptamer, then forming the K^+-stabilized G-quadruplex on the electrode surface, which provides binding sites for EA, thus greatly enhanced the selectivity and sensitivity, with a detection limit of 0.08 nM. The Ap-DNA sensor was successfully challenged in tap water and serum samples. This method enables detection of EA without any chemical modification or fluorescent labeling of the Ap-DNA, which offered a platform for prospective future development of a label-free, simple, sensitive and low-cost assay for the EA detection.

Acknowledgement

We are grateful for financial support from the Open Project of Beijing Research Center for Agricultural Standards and Testing (No. ZBZXKFKT201511), Fund for Innovative Research Group of the National Natural Science Foundation of China (Grant No. 51421065), National Basic Research Program of China (2013CB430405). We also express sincerely thanks to Professor Liang-Hong Guo at the State Key Laboratory of Environmental Chemistry and Eco-toxicology, Research Centre for Eco-environmental Sciences, Chinese Academy of Sciences for his help and constructive suggestions.

Appendix A. Supplementary data

Supplementary data associated with this article can be found, in the online version, at doi:

References

[1] M.C. Poirier, Chemical-induced DNA damage and human cancer risk. Nat. Rev. Cancer, 4 (2004) 630-637.

[2] R.J. Turesky, Heterocyclic aromatic amine metabolism, DNA adduct formation, mutagenesis, and carcinogenesis. Drug Metab. Rev., 34 (2002) 625-650.

[3] O.A. Di Paolo, C.H. Teitel, S. Nowell, B.F. Coles, F.F. Kadlubar, Expression of cytochromes P450 and glutathione S-transferases in human prostate, and the potential for activation of heterocyclic amine carcinogens via acetyl-coA-, PAPS- and ATP-dependent pathways. Int. J. Cancer, 117 (2005) 8-13.

[4] N. Gamage, A. Barnett, N. Hempel, R.G. Duggleby, K.F. Windmill, J.L. Martin, M.E. McManus, Human sulfotransferases and their role in chemical metabolism. Toxicol. Sci., 90 (2006) 5-22.

[5] K.M. Gorlewska-Roberts, C.H. Teitel, J.O. Lay Jr, D.W. Roberts, F.F. Kadlubar, Lactoperoxidase-catalyzed activation of carcinogenic aromatic and heterocyclic amines. Chem. Res. Toxicol., 17 (2004) 1659-1666.

[6] S.M. Cohen, A.R. Boobis, M.E. Meek, R.J. Preston, D.B. McGregor, 4-Aminobiphenyl and DNA reactivity: case study within the context of the 2006 IPCS human relevance framework for analysis of a cancer mode of action for humans. Crit. Rev. Toxicol., 36 (2006) 803-819.

[7] V.G. Vaidyanathan, B.P. Cho, Sequence Effects on Translesion Synthesis of an Aminofluorene-DNA Adduct: Conformational, Thermodynamic, and Primer Extension Kinetic Studies. Biochemistry, 51 (2012) 1983-1995.

[8] A. Gamer, R. Rossbacher, W. Kaufmann, B. van Ravenzwaay, The inhalation toxicity of di-and triethanolamine upon repeated exposure. Food Chem. Toxicol., 46 (2008) 2173-2183.

[9] A.A. Farooqui, S.I. Rapoport, L.A. Horrocks, Membrane phospholipid alterations in Alzheimer's disease: deficiency of ethanolamine plasmalogens. Neurochem. Res., 22 (1997) 523-527.

[10] D.F. Horrobin, The membrane phospholipid hypothesis as a biochemical basis for the neurodevelopmental concept of schizophrenia. Schizophr. Res., 30 (1998) 193-208.

[11] A. Heilkenbrinker, C. Reinemann, R. Stoltenburg, J.G. Walter, A. Jochums, F. Stahl, S. Zimmermann, B. Strehlitz, T. Scheper, Identification of the target binding site of ethanolamine binding aptamers and its exploitation for ethanolamine detection. Anal. Chem., 87 (2015) 677-685.

[12] G. Liang, T. Li, X.H. Li, X.H. Liu, Electrochemical Detection of the Amino-Substituted Naphthalene Compounds Based on Intercalative Interaction with Hairpin DNA by Electrochemical Impedance Spectroscopy. Biosens. Bioelectron., 48 (2013) 238-243.

[13] T.G. Drummond, M.G. Hill, J.K. Barton, Electrochemical DNA sensors. Nat. Biotechnol., 21 (2003) 1192-1199.

[14] J. Liu, Z.H. Wang, G.A. Luo, Q.W. Li, H.W. Sun, The interaction of DNA with dopamine by spectroscopic and electrochemical methods. Anal. Sci., 18 (2002) 751-755.

[15] J. Wang, G. Rivas, X. Cai, E. Palecek, P. Nielsen, H. Shiraishi, N. Dontha, D. Luo, C. Parrado, M. Chicharro, P.A.M. Farias, F.S. Valera, D.H. Grant, M. Ozsoz, M.N. Flair, DNA electrochemical biosensors for environmental monitoring. A review. Anal. Chim. Acta, 347

(1997) 1-8.

[16]K. Kerman, M. Kobayashi, E. Tamiya, Recent trends in electrochemical DNA biosensor technology. Meas. Sci.Technol., 15 (2004) R1-R11.

[17]L.D. Wu, X. Lu, J.B. Jin, H.J. Zhang, J.P. Chen, Electrochemical DNA biosensor for screening of chlorinated benzene pollutants. Biosens. Bioelectron., 26 (2011) 4040-4045.

[18]L. Luo, Z. Zhang, Y. Ding, D. Deng, X. Zhu, Z. Wang, Label-free electrochemical impedance genosensor based on 1-aminopyrene/graphene hybrids. Nanoscale, 5 (2013) 5833-5840.

[19]G. Liang, X.H. Liu, G-quadruplex based impedimetric 2-hydroxyfluorene biosensor using hemin as a peroxidase enzyme mimic. Microchim. Acta, 182 (2015) 2233-2240.

[20]G. Chiti, G. Marrazza, M. Mascini, Electrochemical DNA biosensor for environmental monitoring. Anal. Chim. Acta, 427 (2001) 155-164.

[21]J. Wang, G. Rivas, D. Luo, X. Cai, F.S. Valera, N. Dontha, DNA-Modified Electrode for the Detection of Aromatic Amines. Anal. Chem., 68 (1996) 4365-4369.

[22]J.G. Walter, A. Heilkenbrinker, J. Austerjost, S. Timur, F. Stahl, T. Schepe, Aptasensors for small molecule detection. Naturforsch., 67 (2012) 976-986.

[23]J.L. He, Z.S. Wu, H. Zhou, H.Q. Wang, J.H. Jiang, G.L. Shen, R.Q. Yu, Fluorescence Aptameric Sensor for Strand Displacement Amplification Detection of Cocaine. Anal. Chem., 82 (2010) 1358-1364.

[24]T. Tang, J. Deng, M. Zhang, G. Shi, T. Zhou, Quantum dot-DNA aptamer conjugates coupled with capillary electrophoresis: A universal strategy for ratiometric detection of

organophosphorus pesticides. Talanta, 146 (2016) 55-61.

[25]C. Zhang, L. Wang, Z. Tu, X. Sun, Q. He, Z. Lei, C. Xu, Y. Liu, X. Zhang, J. Yang, Organophosphorus pesticides detection using broad-specific single-stranded DNA based fluorescence polarization aptamer assay. Biosens. Bioelectron., 55 (2014) 216-219.

[26]Y. Xiang, Y. Lu, DNA as sensors and imaging agents for metal ions. Inorg. Chem., 53 (2013) 1925-1942.

[27]N. Mohammad Danesh, M. Ramezani, A. Sarreshtehdar Emrani, K. Abnous, S.M. Taghdisi, A novel electrochemical aptasensor based on arch-shape structure of aptamer-complimentary strand conjugate and exonuclease I for sensitive detection of streptomycin. Biosens. Bioelectron., 75 (2016) 123-128.

[28]B. Strehlitz, C. Reinemann, S. Linkorn, R. Stoltenburg, Aptamers for pharmaceuticals and their application in environmental analytics. Bioanal. Rev., 4 (2012) 1-30.

[29]J. Kosman, B. Juskowiak, Peroxidase-mimicking DNAzymes for biosensing applications: A review. Anal. Chim. Acta, 707 (2011) 7-17.

[30]D. Mann, C. Reinemann, R. Stoltenburg, B. Strehlitz, In vitro selection of DNA aptamers binding ethanolamine. Biochem. Biophys. Res. Commun., 338 (2005) 1928-1934.

[31]Z. Lin, Y. Chen, X. Li, W. Fang, Pb^{2+} induced DNA conformational switch from hairpin to G-quadruplex: electrochemical detection of Pb^{2+}. Analyst, 136 (2011) 2367-2372.

[32]Y. Liu, J. Ren, Y. Qin, J. Li, J. Liu, E. Wang, An aptamer-based keypad lock system. Chem. Commun., 48 (2012) 802-804.

[33]H. Sun, X. Li, Y. Li, L. Fan, H.-B. Kraatz, A novel colorimetric potassium sensor based on

the substitution of lead from G-quadruplex. Analyst, 138 (2012) 856-862.

[34]X.H. Li, Y. Zhou, T.C. Sutherland, B. Baker, J.S. Lee, H.B. Kraatz, Chip-based microelectrodes for detection of single-nucleotide mismatch. Anal. Chem., 77 (2005) 5766-5769.

[35]G. Liang, X.H. Li, X.H. Liu, Electrochemical detection of 9-hydroxyfluorene based on the direct interaction with hairpin DNA. Analyst, 138 (2013) 1032-1037.

[36]G. Liang, X.H. Liu, X.H. Li, Highly sensitive detection of α-naphthol based on G-DNA modified gold electrode by electrochemical impedance spectroscopy. Biosens. Bioelectron. , 45 (2013) 46-51.

[37]H. Gong, T.Y. Zhong, L. Gao, X.H. Li, L.J. Bi, H.B. Kraatz, Unlabeled Hairpin DNA Probe for Electrochemical Detection of Single-Nucleotide Mismatches Based on MutS- DNA Interactions. Anal. Chem., 81 (2009) 8639-8643.

[38]M. Dijksma, B. Boukamp, B. Kamp, W. Van Bennekom, Effect of hexacyanoferrate (II/III) on self-assembled monolayers of thioctic acid and 11-mercaptoundecanoic acid on gold. Langmuir, 18 (2002) 3105-3112.

[39]V. Dharuman, K. Vijayaraj, S. Radhakrishnan, T. Dinakaran, J.S. Narayanan, M. Bhuvana, J. Wilson, Sensitive label-free electrochemical DNA hybridization detection in the presence of 11-mercaptoundecanoic acid on the thiolated single strand DNA and mercaptohexanol binary mixed monolayer surface. Electrochimi. Acta, 56 (2011) 8147-8155.

[40]A. Bogomolova, E. Komarova, K. Reber, T. Gerasimov, O. Yavuz, S. Bhatt, M. Aldissi, Challenges of electrochemical impedance spectroscopy in protein biosensing. Anal. Chem., 81 (2009) 3944-3949.

Figure Captions

Scheme 1. Schematic representation of Ap-DNA for the detection of EA

Fig. 1 The CD spectra of: (a) 25 μM Ap-DNA in Tris-HCl; (b) addition of 25 μM EA to (a); (c) 25 μM Ap-DNA in B-buffer; (d) addition of 25 μM EA to (c).

Fig. 2 Representative Nyquist plots ($-Z_{im}$ *vs*. Z_{re}) for the formed G-quadruplex Ap-DNA films (white circle) before and after interaction with 1.6 mM EA for 1 h (black circle). Measured data were shown as symbols with calculated fit to the equivalent circuit as solid lines. Inset: the measured data were fit to the equivalent circuit; R_s, solution resistance; R_{CT}, charge-transfer resistance; C_{film}, capacitance of the Ap-DNA films; R_x and CPE, resistance and nonlinear capacitor accounting for 6-mercaptohexanol film.

Fig. 3. Sensitivity for EA in B-buffer solution (A): Relationship between ΔR_{CT} and the concentrations of EA. Inset: the magnified section with EA concentrations ranged from 0.08 nM to 160 nM; (B) Linear relationship between ΔR_{CT} and the concentrations of EA ranged from 0.16 nM to 16 nM. The flat horizontal line represents ΔR_{CT} in buffer solution. Error bars are derived from a minimum of three electrodes.

Fig. 4. Selectivity of the Ap-DNA sensor for EA (16 nM) and other selected chemicals (such as 1600 nM ethanol, glycol, isopropanolamine (IPA) and isopropanol) ($\Delta R_{CT} = R_{CT(after)} - R_{CT(buffer)}$); Error bars are derived from a minimum of three electrodes.

Fig. 5 The ΔR_{CT} change for the different concentration of EA after incubation with Ap-DNA films in (A) 10% serum; (B) tap water. (Concentration of EA: 16 nM, 160 nM, 1600 nM)

Table Captions

Table 1. Equivalent Circuit Element Values for The Formed G-quadruplex Ap-DNA Films Before and After Incubating with 1.6 mM EA

Table 1. Equivalent Circuit Element Values for The Formed G-quadruplex AP-DNA Films Before and After Incubating with 1.6 mM EA[a]

	Circuit elements						
	R_s ($\Omega \cdot cm^2$)	C_{film} ($\mu F \cdot cm^{-2}$)	R_{CT} ($\Omega \cdot cm^2$)	R_x ($\Omega \cdot cm^2$)	CPE ($\mu F \cdot cm^{-2}$)	n	ΔR_{CT} ($\Omega \cdot cm^2$)
DNA films	4.4(0.2)	3.2(0.04)	1190.8(59.7)	3.8(0.3)	11.41(0.32)	0.9(0.02)	0
+EA	5.4(0.2)	1.7(0.02)	1603.7(75.3)	1.6(0.2)	10.11(0.41)	0.9(0.03)	412.9(27.4)

[a]The values in parentheses represent the standard deviations from at least three electrode measurements.

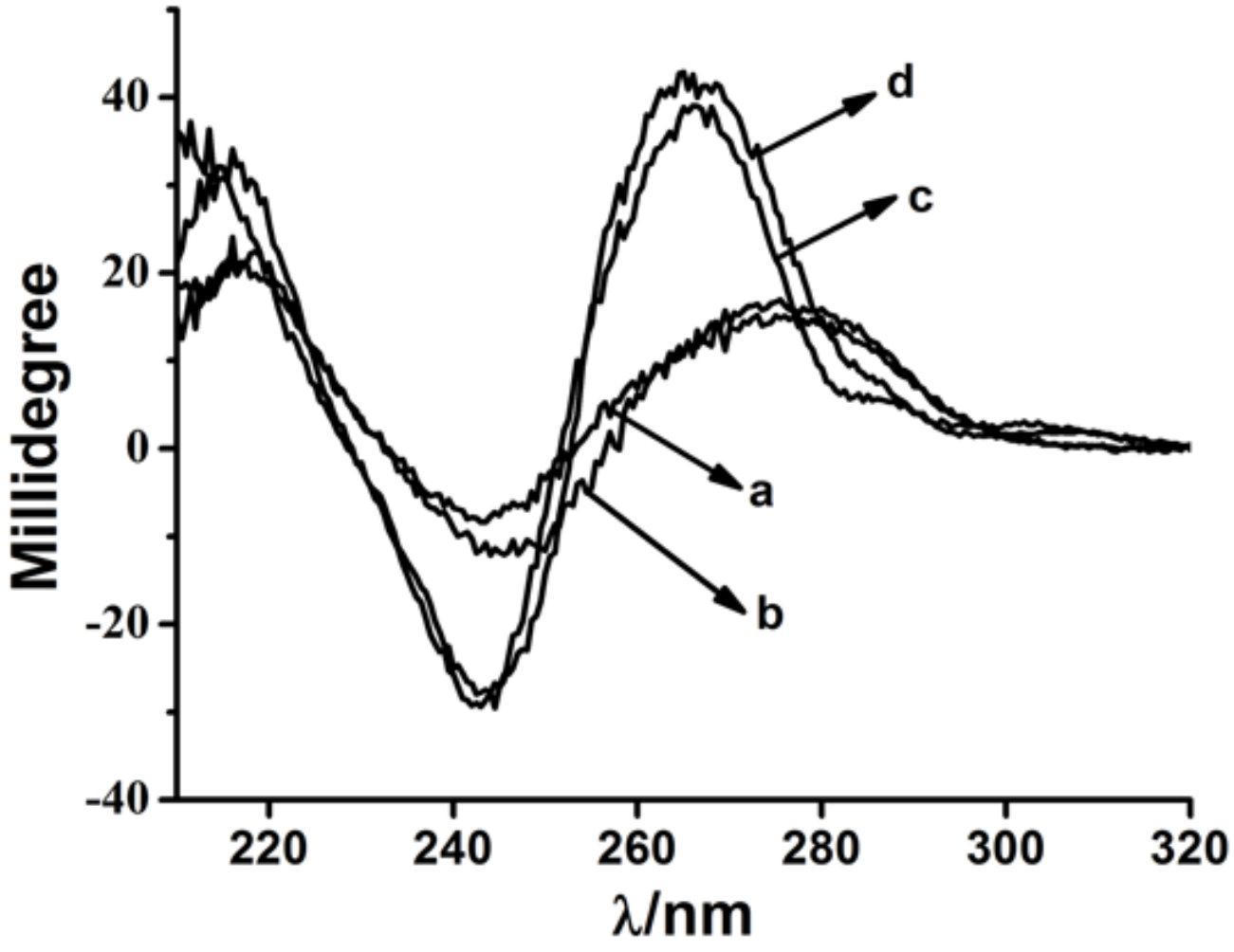
40
20
0
-20
-40
Millidegree
220
240
260
280
300
320
λ/nm
a
b
c
d

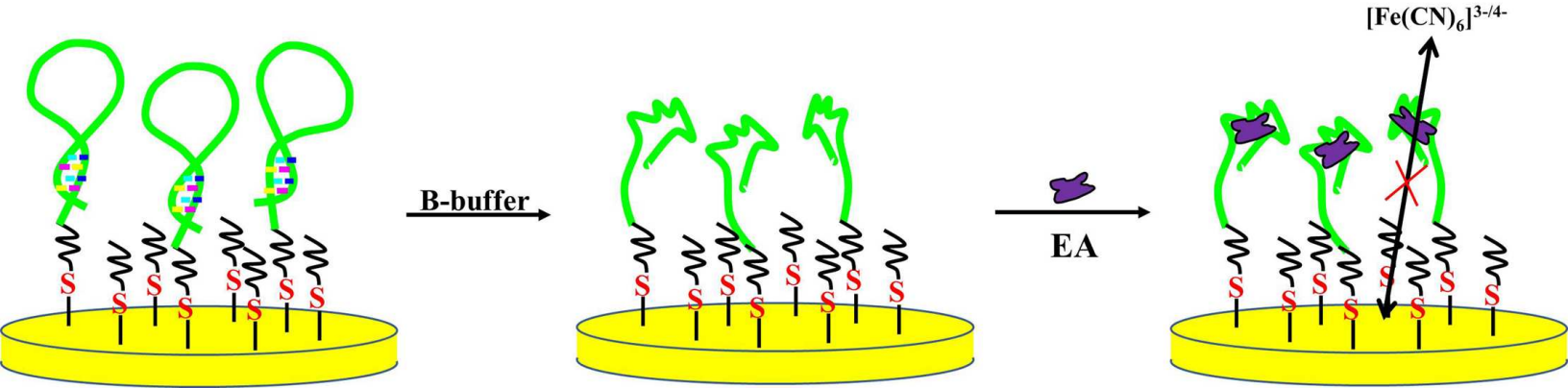

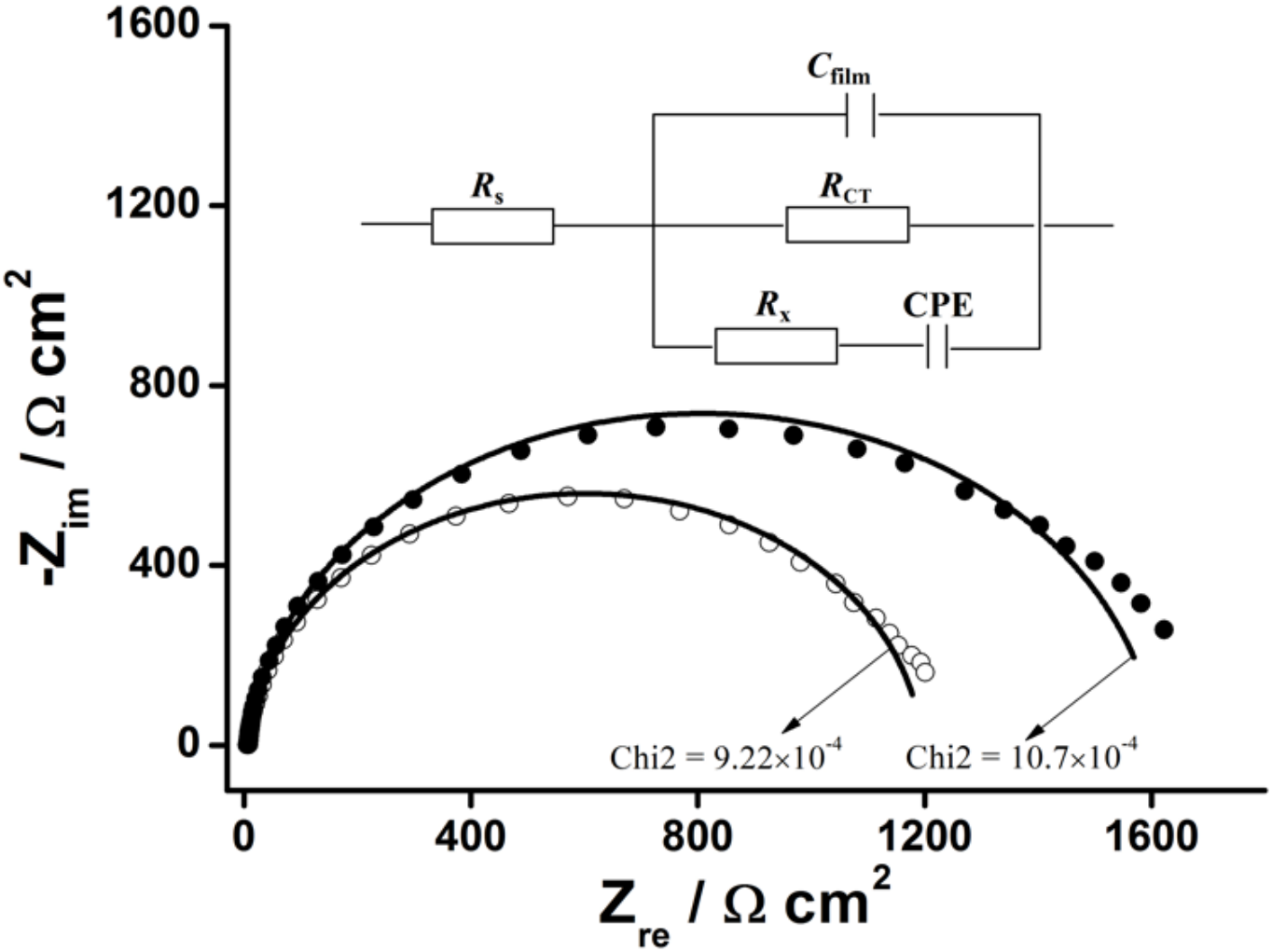
1600
1200
800
400
0
-Z_im / Ω cm^2
0
400
800
1200
1600
Z_re / Ω cm^2
C_film
R_s
R_CT
R_x
CPE
Chi2 = 9.22×10^-4
Chi2 = 10.7×10^-4

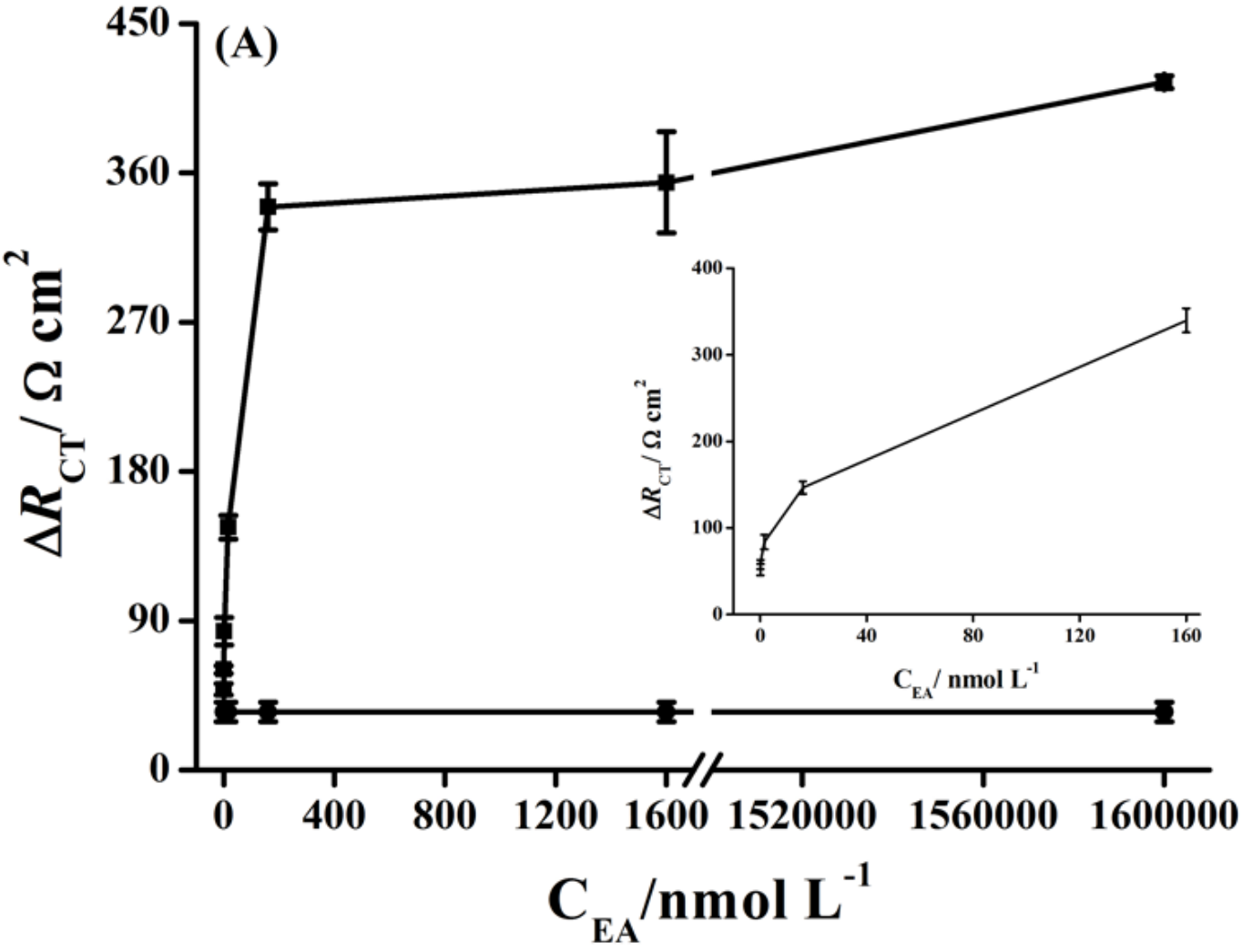
(A)
450
360
270
180
90
0
ΔR_{CT}/ Ω cm^2
0
400
800
1200
1600
1520000
1560000
1600000
C_{EA}/nmol L^{-1}
400
300
200
100
0
ΔR_{CT}/ Ω cm^2
0
40
80
120
160
C_{EA}/ nmol L^{-1}

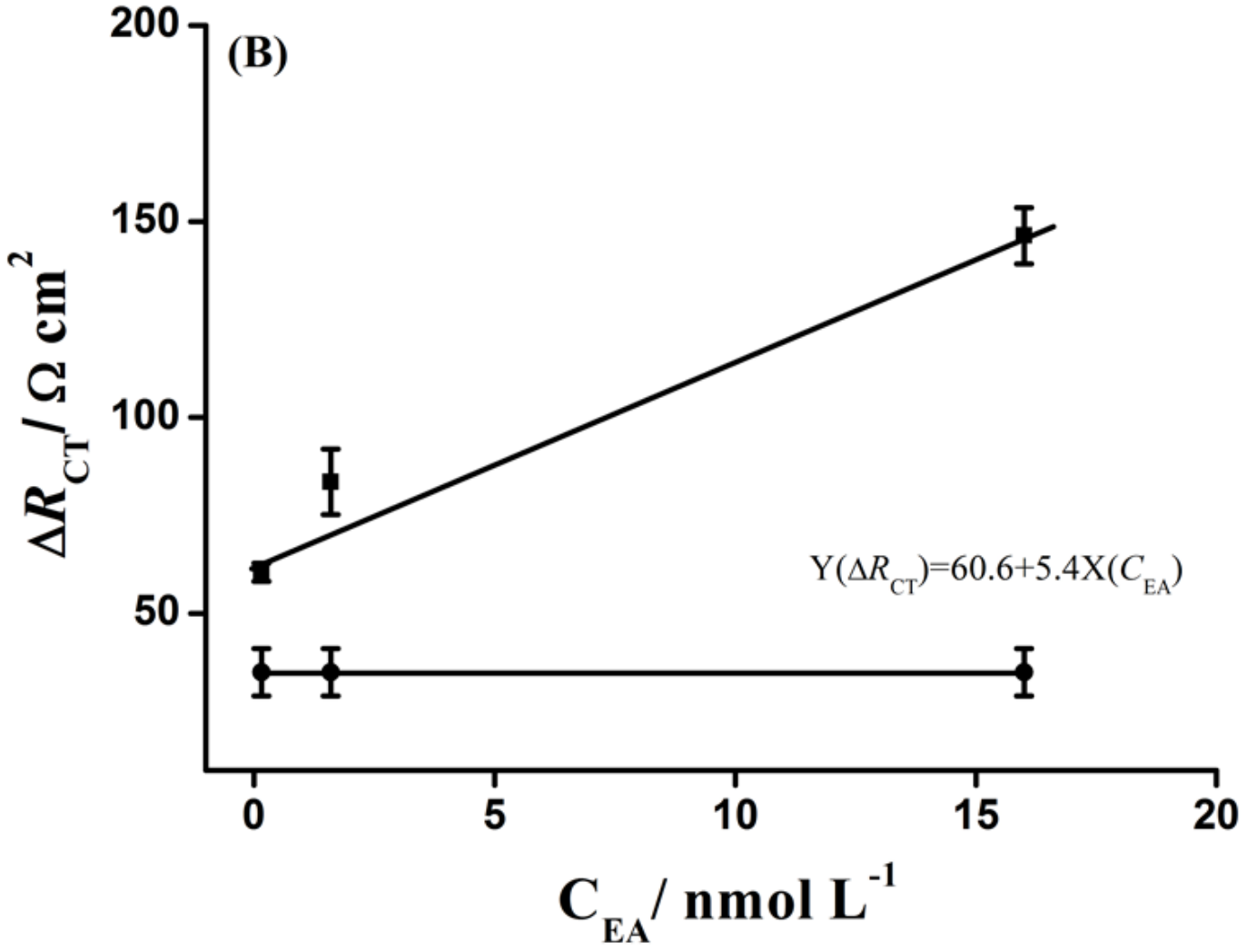
(B)
200
150
100
50
0
5
10
15
20
ΔR_{CT} / Ω cm^2
C_{EA} / nmol L^{-1}
Y(ΔR_{CT})=60.6+5.4X(C_{EA})

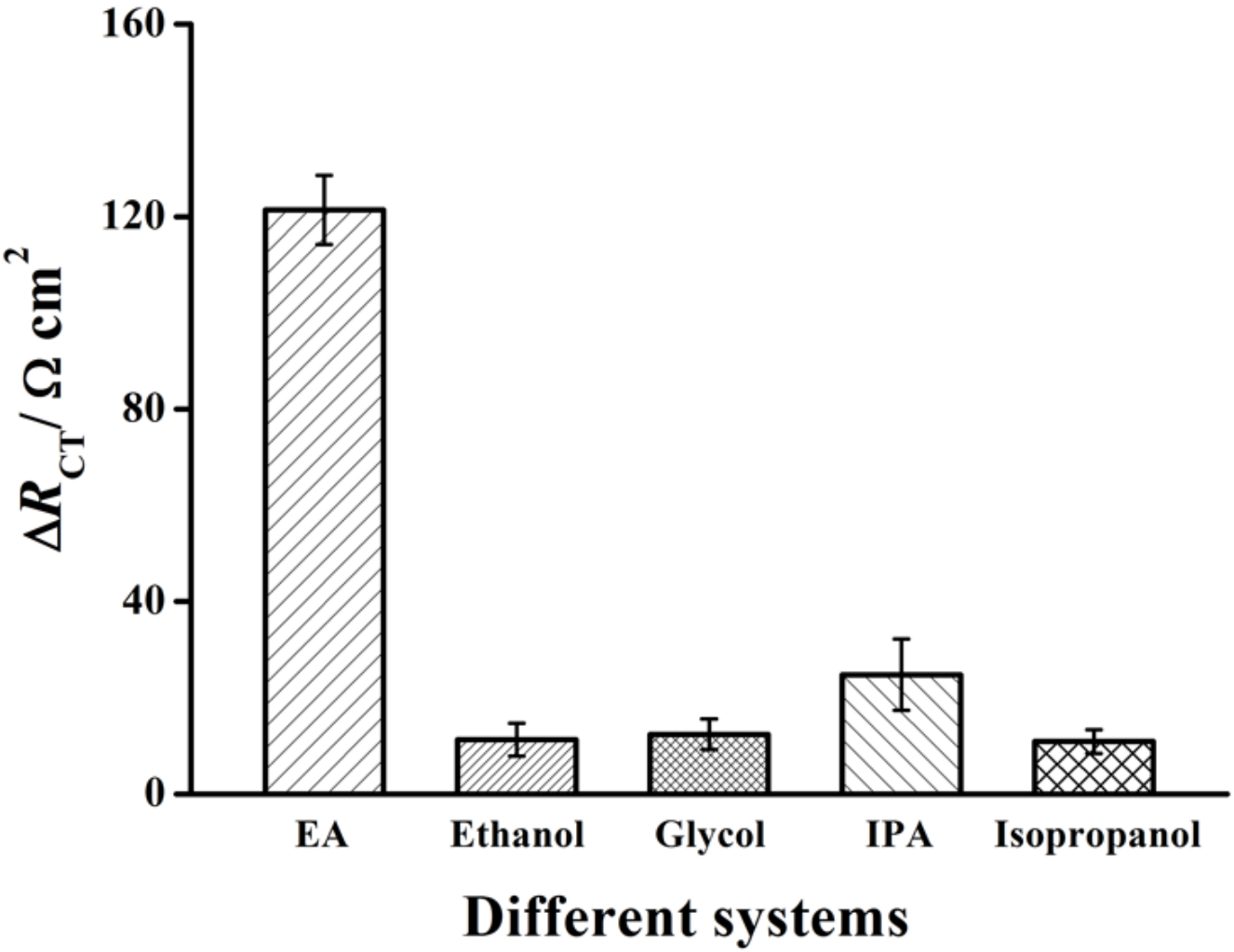

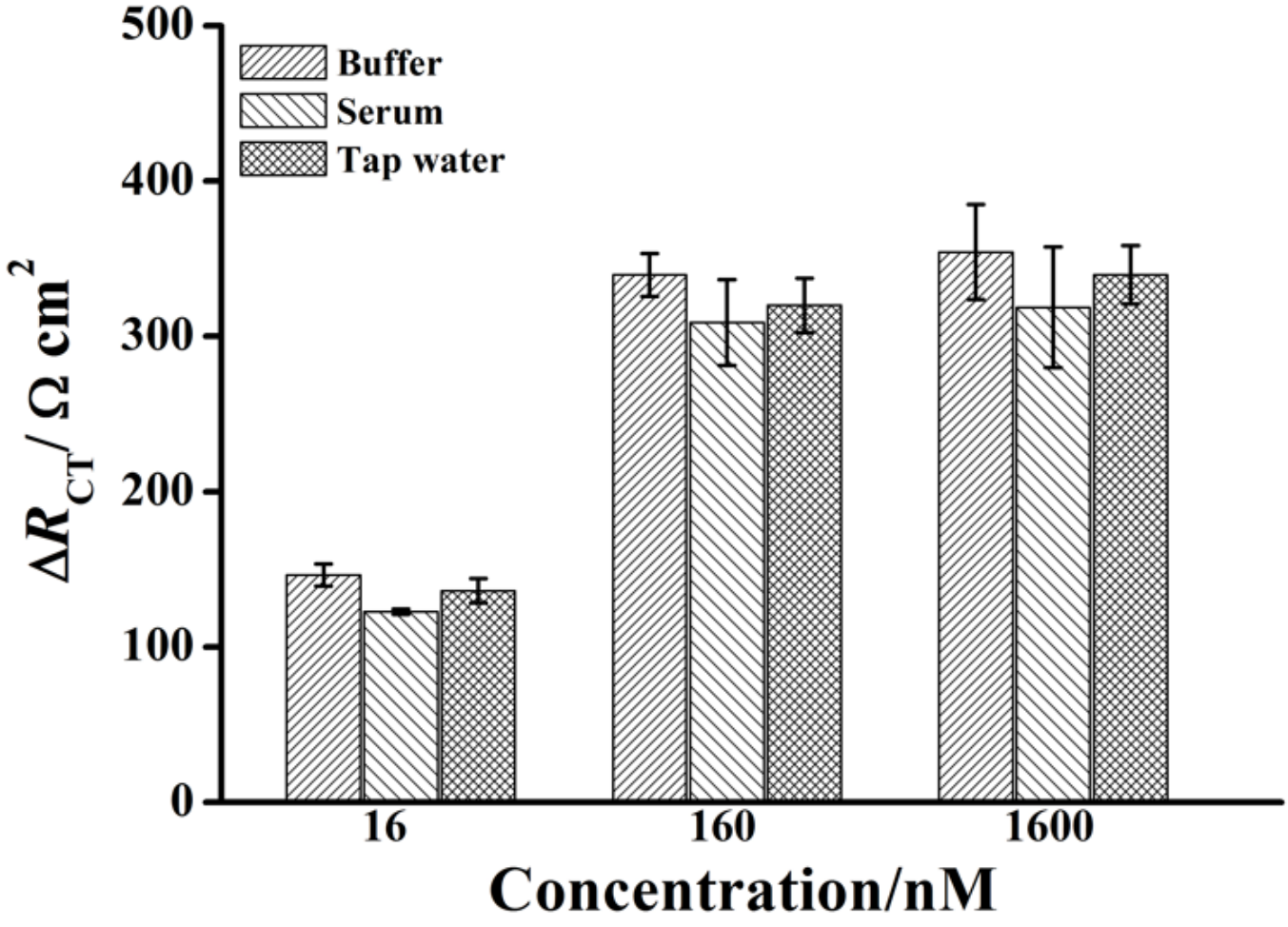
500
400
300
200
100
0
Buffer
Serum
Tap water
ΔR_{CT} / Ω cm^2
16
160
1600
Concentration/nM

Highlights

- Label-free aptamer DNA sensor is developed for EA detection.
- Aptamer switches to G-quadruplex on the electrode, offering the binding site of EA.
- CD and EIS confirm the sensing mechanism.
- The sensor exhibits excellent selectivity and high sensitivity.
- The sensor is successfully challenged in serum and tap water samples.